Use of Local Similarity Concepts in Hypersonic Viscous Interaction Problems

C. Forbes Dewey Jr.*

The Rand Corporation, Santa Monica, Calif.

The problem of predicting the characteristics of a hypersonic laminar boundary layer that interacts with the external flow field is approached using the tangent wedge formulation for the inviscid flow field and the method of similar solutions for the viscous flow. It is shown that the concept of local similarity which allows the pressure gradient parameter β to vary in the streamwise direction leads to an explicit relation between the viscous and inviscid flows for all values of the hypersonic interaction parameter χ_∞. The conditions of "strong" and "weak" interaction appear as asymptotic limits of the general relations. The present theory is compared with three independent experimental investigations. In each case, the agreement is found to be excellent over the range of χ_∞ investigated. It is shown, using asymptotic solutions to the exact boundary layer equations, that the present theory is applicable to a wide variety of viscous interaction problems. A large number of solutions to the laminar boundary layer similarity equations for a perfect gas with cross flow and surface mass transfer are given. These numerical results, when combined with the solutions of previous authors, are sufficient to describe the range of conditions $0 < \beta < 0.4$, $0.15 < t_w < t_{aw}$, $-0.6 \leqslant f'' \leqslant 0$, $0.3 < t_s < 1$, $0.7 < Pr < 1$, $0 < (U_\infty^2/2H_e) < 1$, and $0.5 < \omega < 1$, with high precision.

Nomenclature

a = speed of sound
c_p = specific heat
C_f = skin friction coefficient, Eq. (33)
C_{H_∞} = Stanton number, Eq. (32)
C_∞ = viscosity function, $T_\infty\mu_w/T_w\mu_\infty$
f, g = transformed velocity functions, $f' = u/u_e$, $g = w/w_e$
H = total enthalpy, $c_pT + \frac{1}{2}(u^2 + w^2 + v^2)$
I_1, I_2 = particular integrals across the boundary layer, Eqs. (48) and (49)
k = thermal conductivity
M = Mach number
n = exponent in power law, $p \sim x^n$
p = static pressure
Pr = Prandtl number, $c_p\mu/k$
q = heat flux
$Re_{x,\infty}$ = Reynolds number based on freestream properties, $\rho_\infty U_\infty x/\mu_\infty$
t_s = sweep parameter, Eq. (25)
t_w = normalized wall temperature, T_w/T_0
T = static temperature
T_0 = stagnation temperature
U_∞ = freestream velocity
u, v, w = velocity components in x, y, z directions, respectively
x, y, z = orthogonal body surface coordinates, z being parallel to the leading edge and y being normal to the surface
α, α_e = geometric and effective angles of attack, $\alpha_e = \alpha + (d\delta^*/dx)$
β = pressure gradient parameter
γ = ratio of specific heats
δ^* = boundary layer displacement thickness, Eq. (47)
η, ξ = transformed space variables, Eqs. (11) and (12)
$\mathfrak{C}$ = hypersonic similarity parameter $(M_\infty \cos\Lambda\alpha_e)^{-2}$
$\mathfrak{C}^{(0)}$ = value of $\mathfrak{C}$ far from leading edge
θ = normalized enthalpy function $(H - H_w)/(H_e - H_w)$
Λ = leading edge sweep angle
μ = viscosity
ρ = density
χ_∞ = hypersonic viscous interaction parameter, $M_\infty^3 \cos\Lambda/(Re_{x,\infty})^{1/2}$
ω = exponent in temperature-viscosity relation, $\mu \sim T^\omega$

Subscripts and Superscripts

$(\ )_{aw}$ = evaluated for $\theta_w' = 0$
$(\ )_{e,\,w,\,\infty}$ = evaluated at conditions external to the boundary layer, at the wall, and in the freestream, respectively
$(\ )'$ = derivative with respect to η

I Introduction

THE subject of hypersonic viscous interaction deals with the coupling between the "inviscid" flow field surrounding a high-speed body and the thin viscous layer near the body surface. In conventional aerodynamics, heat transfer, skin friction, and surface pressure are determined using the original idealization of Prandtl; for sufficiently large values of the Reynolds number $\rho ux/\mu$, the flow field is assumed to be composed of two distinct parts: 1) an external field, which is determined by assuming a nonviscous fluid and the boundary condition of no normal velocity at the body surface; and 2) a thin viscous boundary layer near the body which satisfies a no-slip condition at the solid surface and agrees (to the order of the boundary layer approximations) in all dynamic and thermodynamic respects with the local external field at its outer limit. This idealization, that the external field is independent of the boundary layer, has been eminently successful in high Reynolds number flows with but two notable exceptions: first, in regions where, by the combined action of viscous and pressure forces, the flow separates from the surface; and second, in those cases where the local Mach number is sufficiently large that the streamline deflection produced by the boundary layer significantly changes the thermodynamic state of the external flow. In both cases, a coupling exists between the external flow and the viscous motion near the body surface.

Presented at the ARS Space Flight Report to the Nation, New York, October 9–15, 1961; revision received August 9, 1962. Any views expressed in this paper are those of the author. They should not be interpreted as reflecting the views of the Rand Corporation or the official opinion or policy of any of its governmental or private research sponsors.

* Consultant, Aero-Astronautics Department; also National Science Foundation Graduate Fellow, California Institute of Technology, Pasadena, Calif. Member ARS.

Hypersonic viscous interaction has been investigated theoretically by Lees and Probstein,[1] Li and Nagamatsu,[2] and other authors. Bertram,[3] Kendall,[4] and others have provided experimental verification of many features of the theory. The analytic technique used in these investigations is the method of similar solutions. By a suitable transformation of variables, it is possible to reduce the partial differential equations governing the laminar boundary layer to ordinary differential equations of higher order involving a single independent variable; the value of the reduced dependent variables then may be calculated once and for all for any given set of boundary conditions. However, severe restrictions must be placed on the wall temperature, pressure gradient, and mass transfer variation in the streamwise direction to obtain this similarity form, and it is fortuitous if these restrictions are satisfied exactly in real situations.

One method of overcoming this difficulty is to assume a "locally similar" flow; that is, at every streamwise station it is assumed that the boundary layer adjusts instantaneously to changes in the geometric and thermodynamic boundary conditions and is identical in all essential respects to the similar solution boundary layer whose history includes the local boundary conditions. Although this concept has been highly successful in predicting the characteristics of blunt body flows,[5,6] it has not been examined extensively with respect to its usefulness in hypersonic interaction problems. It will be shown that this concept provides a powerful method of treating conditions intermediate to the "exact" solutions represented by "strong" and "weak" viscous interaction.

Solutions of the laminar boundary layer equations with surface mass transfer have been obtained by numerous authors[7–15] in connection with ablation and sublimation cooling schemes for blunt re-entry bodies. It is highly probable that slender hypersonic vehicles also will use this form of heat protection. Accordingly, the present paper investigates the effect of surface mass transfer on the viscous interaction solutions near the leading edge of a swept, lifting surface.

II Governing Equations for the Viscous Flow Field

In this section, a brief derivation of the laminar boundary layer similarity equations is given. The analysis makes use of the well-known Howarth-Dorodnitsyn transformations to reduce the partial differential equations governing compressible viscous boundary layer flow to an equivalent set of coupled nonlinear ordinary differential equations. Since extension of the results of the exact similarity solutions to the case of "locally similar" flows will be of particular interest, the derivation serves primarily to emphasize the restrictions imposed by exact similarity. The formulation is similar to that given by Lees[5] and Reshotko and Beckwith.[14]

Fig. 1 defines the coordinate system under consideration. For a semi-infinite plane surface with leading edge sweep angle Λ, there is no property variation in the z direction. Because of the growth of the boundary layer, the "effective" surface seen by the external flow defines an angle $(\cos\Lambda)\,(\alpha + d\delta^*/dx)$ with respect to the freestream direction. The problem is to calculate the local flow properties (ρ, u, T) by simultaneous solution of the viscous and inviscid flow fields.

The conservation equations for a perfect, homogeneous gas with constant specific heat are reduced to the following form by applying the usual boundary layer approximations:

Continuity

$$[\partial(\rho u)/\partial x] + [\partial(\rho v)/\partial y] = 0 \tag{1}$$

Momentum

$$\rho u \frac{\partial u}{\partial x} + \rho v \frac{\partial u}{\partial y} = -\frac{\partial p}{\partial x} + \frac{\partial}{\partial y}\left(\mu \frac{\partial u}{\partial y}\right) \tag{2}$$

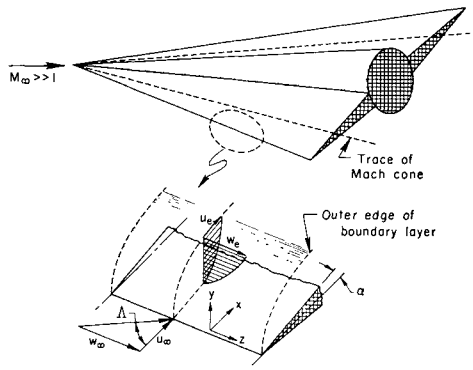

Fig. 1 Leading edge boundary layer coordinates for hypersonic lifting vehicle

$$\rho u \frac{\partial w}{\partial x} + \rho v \frac{\partial w}{\partial y} = + \frac{\partial}{\partial y}\left(\mu \frac{\partial w}{\partial y}\right) \tag{3}$$

$$0 = -(\partial p/\partial y) \tag{4}$$

Energy

$$\rho u \frac{\partial H}{\partial x} + \rho v \frac{\partial H}{\partial y} = \frac{\partial}{\partial y}\left(\frac{\mu}{Pr}\frac{\partial H}{\partial y}\right) - \frac{\partial}{\partial y}\left[\mu\left(\frac{1}{Pr} - 1\right)\frac{\partial}{\partial y}\left(\frac{u^2 + w^2}{2}\right)\right] \tag{5}$$

State

$$p = \rho RT \tag{6}$$

Constitutive

$$Pr = Pr(T) \qquad \mu = \mu(T) \qquad H = c_p T + (u^2 + w^2)/2 \tag{7}$$

Assumptions

$$c_p = \text{const} \qquad v^2 \ll (u^2, w^2) \qquad \partial/\partial y \gg \partial/\partial x \tag{8}$$

Boundary Conditions

$$y = 0 \qquad u = w = 0 \qquad v = v_w \qquad H = H_w \tag{9}$$

$$y \to \infty \qquad u = u_e \qquad w = w_e \qquad H = H_e = c_p T_0 \tag{10}$$

Reduction of Eqs. (1–5) to similarity form is accomplished by introducing the modified Stewartson and Howarth-Dorodnitsyn transformations:

$$\xi(x) = \int_0^x \rho_w \mu_w u_e \, dx \tag{11}$$

$$\eta(x,y) = \frac{u_e}{(2\xi)^{1/2}} \int_0^y \rho \, dy \tag{12}$$

and the new dependent variables (primes denote differentiation with respect to η):

Velocity

$$f' = u/u_e \qquad g = w/w_e \tag{13}$$

Enthalpy

$$\theta = (H - H_w)/(H_e - H_w) \tag{14}$$

The conservation equations, together with the restrictions imposed by similarity, may now be written:

Momentum

$$\frac{d}{d\eta}\left(\frac{\rho\mu}{\rho_w\mu_w} f'\right) + ff'' + \frac{2\xi}{u_e}\frac{du_e}{d\xi}\left(\frac{\rho_e}{\rho} - f'^2\right) = 0 \tag{15}$$

$$d/d\eta[(\rho\mu/\rho_w\mu_w)g'] + fg' = 0 \tag{16}$$

Energy

$$\frac{d}{d\eta}\left(\frac{1}{Pr}\frac{\rho\mu}{\rho_w\mu_w}\theta'\right)+f\theta'+\frac{d}{d\eta}\left\{\left(1-\frac{1}{Pr}\right)\frac{\rho\mu}{\rho_w\mu_w}2\left(\frac{U_\infty^2}{2H_e}\right)\times\frac{1}{(1-t_w)}\left[f''f'\left(\frac{u_e}{u_\infty}\right)^2\cos^2\Lambda+gg'\sin^2\Lambda\right]\right\}=0 \quad (17)$$

Similarity Conditions

$$(2\xi/u_e)(du_e/d\xi)[(\rho_e/\rho)-f'^2]=\phi(\eta) \quad (18)$$

$$Pr=\phi(\eta) \quad (19)$$

$$\rho\mu/\rho_w\mu_w=\phi(\eta) \quad (20)$$

$$\text{Either } u_e/u_\infty=\text{const or } Pr=1 \quad (21)$$

$$H_w=\text{const} \quad (22)$$

$$f_w=\text{const} \quad (23)$$

If $\tan^2\Lambda/M^2$ and α are much less than unity, $u_e/u_\infty=1$ and Eq. (21) is satisfied for all Pr. An adequate approximation for all flight conditions where viscous interaction is important is $u_e/u_\infty=\text{const}\leqslant 1$ for arbitrary Pr. If $Pr=1$, no further statement regarding u_e/u_∞ is required.†

Eq. (18) represents the most severe similarity restriction in that the external flow is allowed to vary only in a prescribed way. This may be seen by introducing the quantities

$$t_w=H_w/H_e=T_w/T_0 \text{ (adiabatic inviscid flow, } c_p=\text{const}) \quad (24)$$

and

$$t_s=\frac{1+[(\gamma-1)/2]M_\infty^2\cos^2\Lambda}{1+[(\gamma-1)/2]M_\infty^2} \quad (25)$$

so that

$$T/T_0=(1-t_w)\theta-(1-t_s)g^2-(u_e/u_\infty)^2\cos^2\Lambda(U_\infty^2/2H_e)f'^2+t_w \quad (26)$$

and

$$\frac{2\xi}{u_e}\frac{du_e}{d\xi}\left[\left(\frac{\rho_e}{\rho}\right)-f'^2\right]=-\frac{2\xi}{u_e}\frac{du_e}{d\xi}\frac{T_0}{T}t_s\left\{f'^2-\frac{1}{t_s}\times[(1-t_w)\theta-(1-t_s)g^2+t_w]\right\} \quad (27)$$

If t_s and t_w are considered free parameters, then the quantity $[(2\xi/u_e)(du_e/d\xi)(T_0/T_e)]$ is required to be a function of η alone. This is satisfied only by special exponential relations between u_e, T_e, and ξ or by a modified Falkner-Skan power law of the form $u_e\sim(T_e/T_0)^{1/2}\xi^m$, where the quantity $\beta=2m$ is equivalent to the Falkner-Skan β but modified as indicated in the foregoing.

The final similarity conditions, Eqs. (22) and (23), require the wall temperature to be constant and the mass flux from the wall to be such that $f_w=\text{const}$. From the definitions of ξ and η,

$$f_w=\left[-\frac{(\rho v)_w}{\rho_w\mu_w u_e}(2\xi)^{1/2}\right]_{\beta=0}=\frac{-v_w}{u_e}\left[\frac{t_s}{\beta}\left(\frac{T_0}{T_e}\right)\left(\frac{\mu_e}{\rho_e u_e}\right)\times\frac{1}{u_e}\frac{du_e}{dx}\right]^{-1/2}_{\beta\neq 0} \quad (28)$$

In summary, the complete specification of the viscous flow field is given by the solution to the following three simultaneous ordinary differential equations with their appropriate transformed boundary conditions:

$$\frac{d}{d\eta}\left(\frac{\rho\mu}{\rho_w\mu_w}f''\right)+ff''-\beta\left\{f'^2-\frac{1}{t_s}[(1-t_w)\theta-(1-t_s)g^2+t_w]\right\}=0 \quad (29)$$

$$d/d\eta[(\rho\mu/\rho_w\mu_w)g']+fg'=0 \quad (16)$$

$$\frac{d}{d\eta}\left(\frac{1}{Pr}\frac{\rho\mu}{\rho_w\mu_w}\theta'\right)+f\theta'+\frac{d}{d\eta}\left\{\left(1-\frac{1}{Pr}\right)\times\frac{\rho\mu}{\rho_w\mu_w}2\left(\frac{U_\infty^2}{2H_e}\right)\frac{1}{(1-t_w)}\left[f''f'\left(\frac{u_e}{u_\infty}\right)^2\times\cos^2\Lambda+gg'\sin^2\Lambda\right]\right\}=0 \quad (17)$$

$$\begin{array}{lllll}\eta=0 & f'=0 & g=0 & \theta=0 & f=f_w=\text{const}\\ \eta\to\infty & f'=1 & g=1 & \theta=1 & \end{array} \quad (30)$$

where Pr, β, f_w, t_w, t_s, $U_\infty^2/2H_e$, and u_e/u_∞ are parameters that depend on freestream conditions, body geometry, and body surface temperature.

Solutions of the similarity equations may be used to calculate the local skin friction and heat transfer. The heat transfer to the body surface is given by

$$q_w=[\rho_w\mu_w u_e/(2\xi)^{1/2}](H_e-H_w)\theta_w' \quad (31)$$

and the local Stanton number is defined by the relation

$$C_{H_\infty}=\frac{q_w}{\rho_\infty U_\infty(H_{aw}-H_w)}=\frac{\cos\Lambda}{(2\tilde{R}e\,Re_{x,e})^{1/2}}\left(\frac{\rho_w\mu_w}{\rho_e\mu_e}\right)^{1/2}\times\frac{\theta_w'}{Pr}\frac{(H_e-H_w)}{(H_{aw}-H_w)}\left(\frac{\rho_e}{\rho_\infty}\right) \quad (32)$$

where $Re_{x,e}=\rho_e u_e x/\mu_e$ and $\tilde{R}e=\left(\int_0^x\rho_w\mu_w u_e dx/\rho_w\mu_w u_e x\right)$ are the appropriate local Reynolds numbers of the flow.

Similarly, the surface friction forces may be written in terms of the local skin friction coefficient as

$$C_f=(2)^{1/2}\left(\frac{u_e}{U_\infty}\right)\left[(f_w'')^2\left(\frac{u_e}{U_\infty}\right)^2+(g_w')^2\left(\frac{w_e}{U_\infty}\right)^2\right]^{1/2}\times(\tilde{R}e\,Re_{x,e})^{1/2}\left(\frac{\rho_w\mu_w}{\rho_e\mu_e}\right)^{1/2}\left(\frac{\rho_e}{\rho_\infty}\right) \quad (33)$$

If θ_w', f_w'', and g_w' are known from the similarity solution and the external flow field found by matching the viscous and inviscid flow fields, the surface observables are determined completely.

III Governing Equations for the Inviscid Flow Field

In this paper, the tangent-wedge approximation to hypersonic small-disturbance theory is used to calculate the inviscid flow field. Cole[17] has derived the hypersonic small-disturbance equations for a swept surface in terms of the following parameters:

$$\Omega=\alpha_e\sin\Lambda \qquad A=[(\alpha)_{\text{shock}}/\alpha_e] \qquad \mathfrak{K}=(M_\infty\alpha_e\cos\Lambda)^{-2} \quad (34)$$

These definitions apply exactly only in the case where $\alpha_e=\alpha$. In using the tangent-wedge approximation $\alpha_e=\alpha+(d\delta^*/dx)$, it is implicitly assumed that $d\alpha_e/dx$ (i.e., the curva-

† It should be emphasized that $u_e=\text{const}$ for an inviscid flow implies that the pressure is also constant, except for stagnation point flows ($u_e=0$) and in the hypersonic limit $U_\infty^2/2H_e\to 1$ for a slender body.

ture of the shock front) is small. As Lees and Probstein[1] have shown, this condition is satisfied as long as $(\delta^*/x)^2 \ll 1$.

The properties downstream of the shock are given by the relations

$$\frac{\rho_e}{\rho_\infty} = \left[\frac{\gamma-1}{\gamma+1} + \frac{2}{\gamma+1}\frac{(1+A^2\Omega^2)}{A^2}\right]^{-1} \tag{35}$$

$$\frac{p_e}{p_\infty} = 1 + \frac{\gamma}{2\mathfrak{K}}\left[\frac{2A}{(1+A\Omega^2)}\right] \tag{36}$$

$$\frac{u_e}{u_\infty} = \frac{A}{(A-1)}\left[\frac{\gamma+1}{\gamma-1} + \frac{p_e}{p_\infty}\right]\left[1 + \frac{\gamma+1}{\gamma-1}\frac{p_e}{p_\infty}\right]^{-1} \tag{37}$$

$$w_e/w_\infty = 1 \text{ everywhere} \tag{38}$$

where Eqs. (35) and (36) are derived by Cole, Eq. (37) is the Rankine-Hugoniot relation, and Eq. (38) follows from the fact that the velocity component parallel to the shock front remains unaltered. The parameter A depends on γ, Ω, and $\mathfrak{K}$ according to the cubic equation

$$\left(\frac{\gamma-1}{2} + \mathfrak{K}\Omega^2\right)\Omega^2A^3 - (1-\mathfrak{K}\Omega^2)A^2 + \left(\frac{\gamma+1}{2} + \mathfrak{K}\Omega^2\right)A + \mathfrak{K} = 0 \tag{39}$$

A may be expanded in powers of Ω by using the asymptotic expansion

$$A = A_0 + \Omega A_1 + \Omega^2 A_2 + \Omega^3 A_3 + \ldots \tag{40}$$

Equating terms of each order of Ω to zero, the following coefficients are obtained:

$$A_0 = \frac{\gamma+1}{4} + \left[\left(\frac{\gamma+1}{4}\right)^2 + \mathfrak{K}\right]^{1/2}$$

$$A_1 = 0 \tag{41}$$

$$A_2 = \frac{[(\gamma-1)/2]A_0^2 + \mathfrak{K}A_0 + \mathfrak{K}}{\{2 - [(\gamma+1)/2A_0]\}}$$

It is easily shown from Eqs. (36, 37, and 41) that u_e/u_∞ is unity to order Ω^2 for all values of $\mathfrak{K}$, provided $\mathfrak{K}\Omega^2$ is of order unity or smaller. The surface pressure may be expressed as

$$\frac{p_e}{p_\infty} = 1 + \frac{\gamma}{2\mathfrak{K}}\left(\frac{\gamma+1}{2} + \left[\left(\frac{\gamma+1}{2}\right)^2 + 4\mathfrak{K}\right]^{1/2} + \Omega^2\left\{\frac{1}{\{1-[(\gamma+1)/4A_0]\}}\left[\frac{\gamma-5}{2}A_0^2 + \left(\frac{\gamma+1}{2} + \mathfrak{K}\right)A_0 + \mathfrak{K}\right]\right\} + \ldots + 0(\Omega^3)\right) \tag{42}$$

For Mach numbers sufficiently large that viscous interaction effects will be important, the corresponding values of Ω will generally be less than $\frac{1}{3}$. The calculations of Feldman[19] show that the velocity ratio across an oblique shock for this range of angles is identical within 5% to the value computed for a perfect gas, even at $M_\infty = 26$ and 250,000 ft altitude. This suggests that any modifications of the theory due to real gas effects will appear in the viscous, rather than the inviscid, part of the solution.[34,35,38]

The pressure gradient parameter β is directly related to the inviscid solution given previously. From (27), one finds that

$$\beta = -\frac{\gamma-1}{\gamma}\left[\left(\frac{t_s}{\cos^2\Lambda}\right)\left(\frac{u_\infty}{u_e}\right)^2\left(\frac{2H_e}{U_\infty^2}\right)\right] \times \frac{\int_0^x \rho_w u_e \mu_w dx}{p_e\rho_w u_e\mu_w}\frac{dp_e}{dx} \tag{43}$$

This form for β may be simplified further for the limiting case of $M^2 \gg 1$, $\Omega^2 \ll 1$, and $\mathfrak{K}\Omega \lesssim 0(1)$:

$$\beta = -\frac{\gamma-1}{\gamma}\frac{\int_0^x p_e dx}{p_e^2}\left(\frac{dp_e}{dx}\right) \tag{44}$$

Similarity conditions are exactly satisfied only if β = const; for example, the limiting cases of "strong" and "weak" interaction may be expressed as follows:

Weak Interaction

$$\mathfrak{K} \to (M_\infty \alpha \cos\Lambda)^{-2} \qquad dp_e/dx \approx 0 \to \beta = 0 \tag{45}$$

Strong Interaction

$$\mathfrak{K} \ll 1 \qquad p_e \sim x^n \to \beta = -[(\gamma-1)/\gamma][n/(n+1)] \tag{46}$$

In the following section, the similarity requirements are discussed in more detail. Eqs. (45) and (46) are included at this point merely to indicate that exact similarity may be obtained only under certain restricted conditions; the two cases cited previously are the only ones that have been treated in the literature in any detail. One interesting observation made by Moore[36] is that, within the thin shock layer approximation ($\gamma \to 1$), $\beta = 0$ for all values of n, as is obvious from (46). Thus, the similarity requirement β = const is satisfied automatically for all values of x if this stringent approximation is made.

IV Matching Relations for Viscous and Inviscid Flow: Application of the Concept of Local Similarity

The tangent wedge approximation assumes that the flow field is uniform between the shock and the edge of the boundary layer.‡ Eqs. (35–38) represent the inviscid solution for ρ_e, p_e, u_e, and w_e behind the shock. These equations involve $\mathfrak{K}$, which in turn depends on the displacement thickness δ^*, and since δ^* itself depends on the external flow, a coupling exists between the viscous and inviscid solutions. The present section defines the nature of this coupling and describes the method of solution using local similarity concepts.

The effective body surface angle is given by $\alpha_e = \alpha + (d\delta^*/dx)$, where

$$\delta^* = \frac{(2\xi)^{1/2}}{\rho_w u_e}\left(\frac{T_0}{T_e}\right)\left[I_1 - \left(\frac{T_e}{T_0}\right)I_2\right] \tag{47}$$

with the definitions

$$I_1 = \int_0^\infty [(1-t_s)\{(1-g^2) - (1-f'^2)\} - (1-t_w)(1-\theta) + (1-f'^2)]d\eta \tag{48}$$

$$I_2 = \int_0^\infty f'(1-f')\,d\eta \tag{49}$$

The two integrals I_1 and I_2 may be evaluated once and for all for any given set of the independent parameters t_s, t_w, $(U_\infty^2/2H_e)$, β, ... In general, I_1 and I_2 will be of the order of unity.

Certain simplifications are available to the hypersonic interaction problem. It was shown in the previous section that the velocity ratio u_e/u_∞ will be nearly unity for a slender body at hypersonic speeds. Furthermore, $T_0/T_e \gg 1$ and

‡ For a simple proof of the fact that the shock wave and boundary layer are distinct in the region where boundary layer concepts are valid, see Hayes and Probstein,[22] p. 336.

Table 1 Similar solutions for $\omega = 1$ and $Pr = 1$[a]

β	t_s	f_w	t_w	f_w''	$\theta_w' = g_w'$	I_1	I_2	$I_1(1)$	$I_1(2)$	$I_1(3)$
0[b]	all	0	0	0.4696	0.4696	0.4696	0.4696	1.686	1.686	1.686
			1.0	0.4696	0.4696	1.686	0.4696	1.686	1.686	1.686
		−0.1414	0	0.3700	0.3700	0.5114	0.5114	1.896	1.896	1.896
			1.0	0.3700	0.3700	1.896	0.5114	1.896	1.896	1.896
		−0.2828	0	0.2766	0.2766	0.5594	0.5594	2.163	2.163	2.163
			1.0	0.2766	0.2766	2.163	0.5594	2.163	2.163	2.163
		−0.3536	0	0.2326	0.2326	0.5862	0.5862	2.326	2.326	2.326
			1.0	0.2326	0.2326	2.326	0.5862	2.326	2.326	2.326
		−0.4243	0	0.1907	0.1907	0.6150	0.6150	2.516	2.516	2.516
			1.0	0.1907	0.1907	2.516	0.6150	2.516	2.516	2.516
		−0.7071	0	0.0502	0.0502	0.7573	0.7573	3.862	3.862	3.862
			1.0	0.0502	0.0502	3.862	0.7573	3.862	3.862	3.862
0.1	1	0	0.15	0.5123	0.4788	0.5910	0.4532	1.658	1.607	1.196
			0.40	0.5347	0.4825	0.8668	0.4480	1.647	1.580	1.188
			0.60	0.5523	0.4854	1.085	0.4438	1.639	1.558	1.182
			1.0	0.5870	0.4909	1.516	0.4355	1.624	1.516	1.170
0.2[c]	1	0	0	0.5233	0.4821	0.3881	0.4457	1.648	1.576	1.188
			0.5	0.6070	0.4951	0.8996	0.4271	1.612	1.480	1.161
			1	0.6867	0.5069	1.392	0.4082	1.580	1.392	1.138
	0.6250	0	0	0.5543	0.4891	0.3878	0.4314	1.627	1.515	1.173
			0.5	0.6836	0.5082	0.8817	0.4041	1.576	1.373	1.134
			1	0.8047	0.5248	1.355	0.3712	1.533	1.247	1.103
	0.3333	0	0	0.6237	0.5039	0.3761	0.3981	1.585	1.383	1.142
			0.5	0.8506	0.5344	0.8479	0.3418	1.508	1.154	1.084
			1	1.058	0.5593	1.287	0.2855	1.450	0.9588	1.042
0.2857[d]	1	0	0	0.5427	0.4874	0.3646	[e]	[e]	[e]	[e]
			0.2	0.5890	0.4940	0.5571				
			0.4	0.6330	0.4983	0.7499				
			0.6	0.6779	0.5069	0.9389				
			0.8	0.7200	0.5050	1.125				
			1.0	0.7633	...	1.306			[f]	
		−0.2	0	0.4033	0.3512	0.3932				
			0.2	0.4548	0.3604	0.6174				
			0.4	0.5043	0.3690	0.8365				
			0.6	0.5522	0.3771	1.050				
			0.8	0.5980	0.3750	1.237				
			1.0	0.6437	...	1.460			[f]	
		−0.4	0	0.2759	0.2302	0.4257				

Eq. (47) may be simplified to

$$\frac{\delta^*}{x} = \frac{(\gamma - 1)}{2^{1/2}} \frac{\rho_w \mu_w}{\rho_e \mu_e} \frac{M_e^2 (\tilde{R}e)^{1/2}}{(Re_{x,e})^{1/2}} I_1 \qquad (50)$$

In the remainder of this paper, Eq. (50) and the approximations $M_e^2 \gg 1$, $u_e = u_\infty$, $\Omega^2 \ll 1$, and $\tan^2\Lambda/M_\infty^2 \ll 1$ will be used unless otherwise noted. This formulation is consistent with the use of hypersonic small disturbance theory and simplifies the computations considerably. The quantities I_1, I_2, and three additional integrals are tabulated in the Appendix to facilitate computation of the local boundary layer profile parameters and the error in the neglected term of (47).

It is interesting to note that the effects of sweep appear directly in the evaluation of I_1 and indirectly in the evaluation of the local external flow field. It was shown earlier using an expansion in the parameter $\Omega = \alpha_e \sin\Lambda$ that, to terms of order Ω^2, the external flow field is identical to that for an unswept surface with the same value of $\mathfrak{IC}$; thus, for $\Omega^2 \ll 1$, $d\delta^*/dx$ for swept and unswept surfaces will differ only in the value of I_1. From Eqs. (16, 29, and 48), the magnitude of this effect may be shown to be small.

Before calculating $d\delta^*/dx$ and completing the matching relations, it is important to discuss the conditions under which local similarity concepts may be applied. As stated previously, exact solutions to the viscous equations may be obtained for β, t_w, Pr, ω, $U_\infty^2/2H_e$, u_e/u_∞, f_w, and t_s const. For example, consider β to be a function of x, holding the remaining parameters fixed. The pressure gradient term of the transformed momentum equation is of order $\beta(t_w/t_s)$ at the wall and identically zero at the outer edge of the boundary layer;[23] from this observation, it might be expected (and indeed is confirmed by the calculations) that I_1, I_2, and the derivatives f_w'', g_w', θ_w' are slowly varying functions of β if either β or t_w is small. In order for the value of any of the foregoing quantities, say Q_i, to be given accurately by the similarity equations, it is necessary that [$\beta = \beta(\xi)$]

$$\Psi(Q_i) = \frac{\xi}{Q_i}\frac{dQ_i}{d\xi} = \left(\frac{\xi}{\beta}\frac{d\beta}{d\xi}\right)\left(\frac{\beta}{Q_i}\frac{dQ_i}{d\beta}\right) \ll 1 \qquad (51)$$

Lees[5] has shown that, for a highly cooled blunt body, the quantities $df_w''/d\beta$, $d\theta'/d\beta$, etc., are sufficiently small that one may, to a good approximation, simply take $\beta = 0$. In the case of viscous interaction with $\gamma \neq 1$ and t_w not necessarily small, the inequality of (51) must be re-examined. This is done in the following section.

The local similarity approximation makes use of the fact that β is a slowly varying function of x. Eq. (46) is used to compute the local value of β; from the condition $p \sim x^n$, one has

$$n = \frac{x}{p}\frac{dp}{dx} = \left(\frac{\mathfrak{IC}}{p}\frac{dp}{d\mathfrak{IC}}\right)\left(\frac{x}{\mathfrak{IC}}\frac{d\mathfrak{IC}}{dx}\right) \qquad (52)$$

The first term in parentheses may be evaluated using the

Table 1 (*Continued*)

β	t_s	f_w	t_w	f_w''	$\theta_w' = g_w'$	I_1	I_2	$I_1(1)$	$I_1(2)$	$I_1(3)$
			0.2	0.3336	0.2424	0.6821				
			0.4	0.3878	0.2534	0.9374				
			0.6	0.4391	0.2623	1.178				
			0.8	0.4888	0.2720	1.411				
			1.0	0.5365	...	1.639			[f]	
		−0.6	0	0.1630	0.1273	0.4591				
			0.2	0.2280	0.1435	0.7740				
			0.4	0.2869	0.1568	1.059				
			0.6	0.3415	0.1681	1.336				
			0.8	0.3934	0.1782	1.592				
			1.0	0.4428	...	1.853			[f]	
0.4[d]	1	0	0	0.5641	0.4905	0.3347				
			0.2	0.6260		0.5224				
			0.4	0.6854		0.6989				
			0.6	0.7432		0.8754				
			0.8	0.7990		1.037				
			1.0	0.8550	...	1.211			[f]	
		−0.2	0	0.4246	0.3565	0.3582	[e]	[e]	[e]	[e]
			0.2	0.4923		0.5732				
			0.4	0.5571		0.7709				
			0.6	0.6194		0.9682				
			0.8	0.6795		1.159				
			1.0	0.7377		1.347			[f]	
		−0.4	0	0.2960	0.2363	0.3819				
			0.2	0.3710		0.6464				
			0.4	0.4413		0.8558				
			0.6	0.5077		1.044				
			0.8	0.5711		1.286				
			1.0	0.6319		1.500			[f]	
		−0.6	0	0.1809	0.1340	0.4113				
			0.2	0.2647		0.6968				
			0.4	0.3399		0.9380				
			0.6	0.4097		1.201				
			0.8	0.4756		1.431				
			1.0	0.5382		1.669			[f]	

[a] These results hold for all values of $\sigma_2 = (U_\infty^2/2He)(ue/u_\infty)^2$.
[b] From Ref. 10; all quantities linear in t_w.
[c] From Ref. 15.
[d] From Ref. 13; see also Ref. 33, where results for $t_s < 1$ are presented.
[e] These quantities not available.
[f] $I_1 = I_1(2)$ for $t = t = 1$.

tangent wedge relation for $\Omega^2 \ll 1$ given by Eq. (42). The second term may be written as

$$\frac{x}{\mathfrak{IC}}\frac{d\mathfrak{IC}}{dx} = -\frac{2x}{\alpha_e}\frac{d\alpha_e}{dx} \qquad \alpha_e = \alpha + \frac{d\delta^*}{dx} \tag{53}$$

and, for $p \sim x^n$ with $t_w = \text{const}$,

$$\frac{d\delta^*}{dx} = \frac{(1-n)}{[2(1+n)]^{1/2}}\left(\frac{\gamma-1}{2}\right)\left(\frac{\rho_w\mu_w}{\rho_\infty\mu_\infty}\right)^{1/2} \times I_1 \frac{M_\infty^3}{(Re_{x,\infty})^{1/2}} \sim x^{-[(1+n)/2]} \tag{54}$$

Eqs. (42, 53, and 54) lead to the following explicit relation between n and $\mathfrak{IC}$:

$$n = -\frac{[1-(\mathfrak{IC}/\mathfrak{IC}^{(0)})^{1/2}]B}{1+[1-(\mathfrak{IC}/\mathfrak{IC}^{(0)})^{1/2}]B}$$

$$B = \frac{\gamma\{[(\gamma+1)/2]+C\} - (2\gamma\mathfrak{IC}/C)}{\gamma\{[(\gamma+1)/2]+C\} + 2\mathfrak{IC}} \tag{55}$$

$$C = \{[(\gamma+1)/2]^2 + 4\mathfrak{IC}\}^{1/2}$$

$$\mathfrak{IC}^{(0)} = (M_\infty \cos\Lambda\alpha)^{-2}$$

The variations of $n(\gamma, \mathfrak{IC}, \mathfrak{IC}^{(0)})$ and $\beta(\gamma, \mathfrak{IC}, \mathfrak{IC}^{(0)})$ with $\mathfrak{IC}$ for $\gamma = 1.4$ are shown in Fig. 2. $\mathfrak{IC}^{(0)}$ is simply a measure of the geometrical slope of the body surface; far from the leading edge, $\mathfrak{IC} \to \mathfrak{IC}^{(0)}$.

From Eqs. (42) and (55), both the viscous and inviscid regions are completely determined for every value of $\mathfrak{IC}$. Since $I_1 = I_1(\beta) = I_1(\mathfrak{IC})$, the local surface pressure may be expressed as a unique function of the viscous interaction parameter $C_\infty^{1/2}\chi_\infty$ by using the relation

$$\frac{1}{\mathfrak{IC}^{1/2}} = \frac{1}{\mathfrak{IC}^{(0)1/2}} + \frac{(1-n)}{[2(1+n)]^{1/2}}\left(\frac{\gamma-1}{2}\right) I_1 \times \left(\frac{p_e}{p_\infty}\right)^{1/2} C_\infty^{1/2}\chi_\infty$$

$$\chi_\infty = \frac{M_\infty^3 \cos\Lambda}{(Re_{x,\infty})^{1/2}} \qquad C_\infty = \frac{T_\infty}{T_w}\frac{\mu_w}{\mu_\infty} \tag{56}$$

This formulation is valid for all values of χ_∞, provided that the similarity criteria (51) is satisfied and the boundary layer and tangent-wedge relations hold.

The present analysis may be compared to previous solutions by taking the limits of Eq. (50) as $\mathfrak{IC} \to 0$ and $\mathfrak{IC} \to \mathfrak{IC}^{(0)}$:

$$\underset{\mathfrak{IC} \to \mathfrak{IC}^{(0)}}{\text{"weak" interaction}} \frac{\delta^*}{x} = \left(\frac{\gamma-1}{2}\right)\frac{M_e^2}{(Re_{x,e})^{1/2}} \times \left(\frac{\rho_w\mu_w}{\rho_e\mu_e}\right)^{1/2} I_1 \tag{57}$$

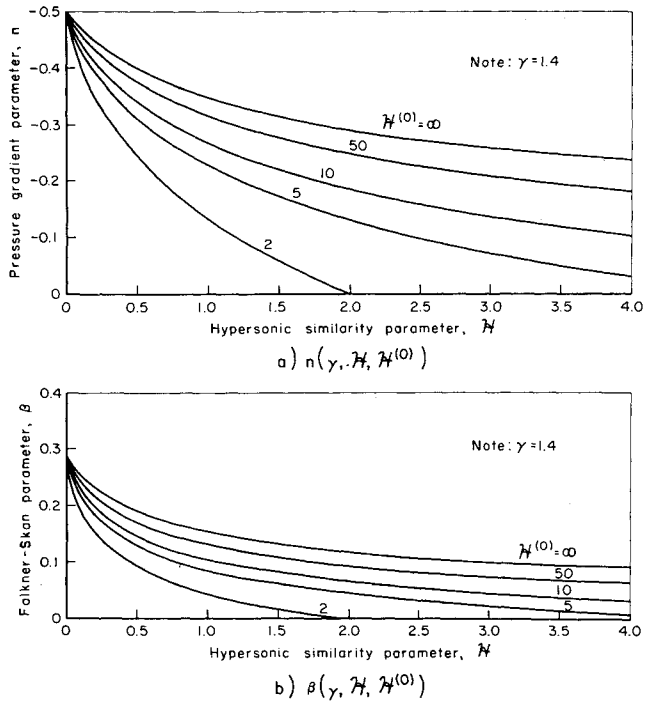

Fig. 2 Variation of the pressure gradient parameters β and n with $\mathcal{H}$

$$\underset{\mathcal{H}\to 0}{\text{"strong" interaction}} \frac{\delta^*}{(x/\cos\Lambda)} = \frac{[\chi_\infty (C_\infty)^{1/2}]^{1/2}}{M_\infty}\left[\frac{4}{3}\frac{(\gamma-1)}{[\gamma(\gamma+1)]^{1/2}}\,2^{1/2}I_1\right]^{1/2} \quad (58)$$

in agreement with Eqs. (9.2.5a,b) and (9.3.13) of Ref. 22. The form of the equation for the induced pressure in the strong interaction limit may be written ($\Lambda = 0$)

$$\frac{p_e}{p_\infty} = \left(\frac{\gamma-1}{4}\right) 2^{1/2} I_1\, C_\infty{}^{1/2} \frac{M_\infty{}^3}{(Re_{x,\infty})^{1/2}} \times \left\{\frac{3}{2}\,[\gamma(\gamma+1)]^{1/2}\right\} \quad (59)$$

The results of Cheng et al.[28] which are based on the thin shock layer approximation $\gamma \to 1$ reduce to (59) for negligible bluntness, except that the term in braces is replaced by $[2\gamma 3^{1/2}/(\gamma + 1)]$. Although the qualitative variation with $C_\infty{}^{1/2}\chi_\infty$ is the same for both formulations, the predicted pressure differs by about 20% for $\gamma = 1$, and the agreement becomes progressively worse with increasing γ. Since the pressure enters as $(p_e/p_\infty)^{1/2}$ in the heat transfer relation, Cheng's formulation would predict a heat transfer coefficient C_{H_∞} about 10% below the present solution (using the same values of I_1 and θ_w').

With the pressure ratio p_e/p_∞ and χ_∞ known, the local Stanton number may be found from

$$M_\infty{}^3 C_{H\infty} = \left(\frac{1+n}{2}\right)^{1/2} \frac{\theta_w'}{Pr}\frac{(1-t_w)}{(t_{aw}-t_w)}\left(\frac{p_e}{p_\infty}\right)^{1/2} C_\infty{}^{1/2}\chi_\infty \quad (60)$$

where $\theta_w' = \theta_w'(\beta) = \theta_w'(\mathcal{H})$. The local skin friction may be determined similarly using (33). Extension of the local similarity approximation to include cases where f_w and t_w vary in the x direction may be handled in an analogous manner, but (56) must be solved by iteration for each value of $\chi_\infty(x)$, since $I_1 = I_1(x, \mathcal{H})$.

In summary, simultaneous solution of the inviscid and viscous flow regimes may be accomplished for all values of the interaction parameter χ_∞ using only two basic assumptions; these are 1) the tangent-wedge approximation adequately represents the exact solution to the inviscid flow field, and 2) the boundary layer is everywhere "locally similar"; that is [see Eq. (51)], $\Psi(I_1)$, $\Psi(\theta_w')$, and $\Psi(f_w'')$ are much less than unity.

V Adequacy of the Approximations

The tangent-wedge approximation has been questioned on numerous occasions (cf. Refs. 1, 21, and 22), and no general criteria are available for evaluating the errors involved in this simplification. The usual approach is to examine only hypersonic small-disturbance theory itself, from which the tangent-wedge relations are derived, and assume that the difference between the tangent-wedge and small-disturbance results is negligible. On the basis of the limited information available, this approach appears to be reasonably adequate. Further investigation of this question is certainly required, following the guidelines laid down by Mirels[39] and Mirels and Thornton.[40]

A rigorous justification of the local similarity approximation to the boundary layer equations is a matter of great importance. In most cases of engineering interest (the present problem being a typical example), one or more of the similarity conditions (18–23) are violated. The question then arises: what estimate may be made of the error incurred in using the *local* similarity solutions defined by the *local* values of β, t_w, . . . ? The complete problem is quite involved, and only the elements germane to the present investigation are considered here. A general formulation is being developed by the author and Toshi Kubota of the California Institute of Technology.

The point $x = 0$ is a singular point of the boundary layer equations, and in hypersonic flow the equations fail in the vicinity of the leading edge.[16,20,26] Further downstream, in the strong interaction region, a similar solution exists for the boundary layer equations, with $\beta = (\gamma - 1)/\gamma \neq 0$ for $\gamma \neq 1$. Provided that the region of validity of the strong interaction limit is nonvanishing,[§] a power series expansion of the form

$$\beta(\xi) = \sum_k \beta_k \xi^k$$

may be constructed around the point $\xi = 0$, as originally detailed by Görtler.[42] Alternatively, the "principal function" $\beta(\xi)$ may be inverted to yield $\xi(\beta)$. This inversion, given by Merk[43] in his treatment of Meksyn's method, will prove to be of crucial importance since the expansions of interest here are for values of $\xi \neq 0$.

For the sake of simplicity, consider the momentum equation (29) with $t_w = t_s = 1$, $f_w = 0$, and $\rho\mu$ const. The nonsimilar form of this equation for $f(\xi,\eta)$ may be written (primes denote differentiation with respect to η)

$$f''' + ff'' + \beta(\xi)(1 - f'^2) = 2\xi \frac{\partial(f',f)}{\partial(\xi,\eta)} \quad (61)$$

and is subject to the boundary conditions

$$f(\xi,0) = f'(\xi,0) = 0 \qquad f'(\xi,\infty) = 1 \quad (62)$$

Using the inversion $\xi = \xi(\beta)$, the Jacobian on the right-hand side of (61) reads

$$2\xi \frac{\partial(f',f)}{\partial(\xi,\eta)} \equiv 2\xi \frac{d\beta}{d\xi}\frac{\partial(f',f)}{\partial(\beta,\eta)}$$

so that

$$f''' + ff'' + \beta(1 - f'^2) = 2\xi(\beta)\frac{d\beta}{d\xi}\frac{\partial(f',f)}{\partial(\beta,\eta)} \quad (63)$$

§ The existence of a true strong interaction region may be shown (from Refs. 18 and 41 and the data of Refs. 24 and 25) to require $C_\infty{}^{1/2}\chi_\infty \gtrsim 10$, whereas $M/(Re_{\infty,x})^{1/2} \lesssim 0.1$.

Eq. (63) shows that the local similarity approach will be valid if the right-hand side is everywhere small. This suggests that an appropriate asymptotic expansion for any value of β is

$$f(\xi,\eta) \equiv f(\beta;\eta) = f_0(\beta;\eta) + \epsilon f_1(\beta;\eta) + \dots \quad (64)$$

with

$$\epsilon = 2\,\xi(\beta)(d\beta/d\xi) \quad (65)$$

The functions f_0 and f_1 satisfy the following differential equations and boundary conditions:

Zeroth Order in ϵ

$$\left.\begin{aligned} &f_0''' + f_0 f_0'' + \beta(1 - f_0'^2) = 0 \\ &f_0(\beta;0) = f_0'(\beta;0) = 0 \qquad f_0'(\beta;\infty) = 1 \end{aligned}\right\} \quad (66)$$

First Order in ϵ

$$\left.\begin{aligned} &f_1''' + f_0 f_1'' - 2\beta f_0' f_1' + f_0'' f_1 = \partial(f_0', f_0)/\partial(\beta,\eta) \\ &f_1(\beta;0) = f_1'(\beta;0) = f_1'(\beta;\infty) = 0 \end{aligned}\right\} \quad (67)$$

The zeroth order solution is simply the similar solution at the point in question. It has an expansion near $\eta = 0$ of the form

$$f_0(\beta;\eta) = \sum_{k=0} \frac{a_k}{k!}\,\eta^k \quad (68)$$

By using (68) in (67), a similar expansion for f_1 may be found:

$$f_1 = f_1''(0) \sum_k \frac{b_k}{k!}\,\eta^k \quad (69)$$

where

$$b_0 = b_1 = b_3 = b_4 = 0 \qquad b_2 = 1$$

$$b_5 = 2f_0''(0)(2\beta - 1) + [f_0''(0)/f_1''(0)]\,[df_0''(0)/d\beta] \quad (70)$$

$$b_6 = 4\beta(1 - \tfrac{3}{2}\beta) - 2[f_0''(0)/f_1''(0)]$$

$$b_7 = 2\beta/f_1''(0) \qquad b_8 = \dots$$

The quantity $f_1''(0)$ depends only on β and is determined by satisfying the boundary condition $f_1'(\beta;\infty) = 0$. Preliminary calculations indicate $f_1''(0) \approx \frac{1}{4} f_0''(0)$ for $\beta = \frac{1}{2}$.

An examination shows that the solution of the homogeneous equation corresponding to (67) meeting the boundary conditions $f_1(\beta;0) = f_1'(\beta;0) = f_1'(\beta;\infty) = 0$ is $f_1 = 0$. Thus, if the Jacobian is small (as it would be in the equivalent problem with a highly cooled wall), one would expect that $f_1''(0) \ll f_0''(0)$. Low[46] has studied several linear equations that are similar to (67) but with different inhomogeneous terms. From his work, one may infer that, for $\beta \geqslant 0$,

$$|f_1''|_{\max} \sim 0[\partial(f_0', f_0)/\partial(\beta,\eta)] = 0(df_0''/d\beta) \quad (71)$$

Then, using the definition (51) and the asymptotic representation (64) of f,

$$f''(0) = f_0''(0)\left[1 + 0\left(\frac{\epsilon}{f_0''(0)}\,\frac{df_0''(0)}{d\beta}\right)\right]$$

$$= f_0''(0)[1 + 0\{\Psi[f_0''(0)]\}] \quad (72)$$

where

$$\Psi[f_0''(0)] = \left(\frac{\xi}{\beta}\frac{d\beta}{d\xi}\right)\left(\frac{\beta}{f_0''(0)}\,\frac{df_0''(0)}{d\beta}\right)$$

A generalization of this result would be

$$\Psi(Q_i) = D[(\beta/Q_i)(dQ_i/d\beta)] \quad (51)$$

where

$$D = [(\xi/\beta)(d\beta/d\xi)]$$

In the present problem, the quantity D may be evaluated explicitly. It may be found from Eqs. (44) and (53) that

$$D(\gamma,\mathcal{H},\mathcal{H}^{(0)}) = -\frac{1}{2}\left\{\left(\frac{\mathcal{H}}{\mathcal{H}^{(0)}}\right)^{1/2} + 4\left[1 - \left(\frac{\mathcal{H}}{\mathcal{H}^{(0)}}\right)^{1/2}\right]\frac{\mathcal{H}}{C^2} \times \left[\left\langle \frac{C^2 + [\gamma(\gamma+1)/2] + 2C\gamma + 2\mathcal{H}}{[\gamma(\gamma+1)/2] + C\gamma + 2\mathcal{H}} \right\rangle - \left\langle \frac{[\gamma(\gamma+1)/2] + C\gamma}{[\gamma(\gamma+1)/2] + C\gamma - (2\gamma\mathcal{H}/C)} \right\rangle\right]\right\} \quad (73)$$

where $C(\gamma,\mathcal{H})$ is defined in Eq. (55). The function $D(\gamma,\mathcal{H},\mathcal{H}^{(0)})$ is shown in Fig. 3a for $\gamma = 1.4$; it may be shown that $D \to 0$ as $\mathcal{H} \to 0$ and $D \to -\frac{1}{2}$ as $\mathcal{H} \to \mathcal{H}^{(0)}$. The important point here is that D is identically zero in the region of strong interaction and in the weak interaction limit approaches a constant value of order one. If the numerical solutions of the perturbation equations give values for the quantity $(\beta/Q_i)(dQ_i/d\beta)$, or more correctly $\beta(Q_i)_1/(Q_i)_0$, which are of order one or less in the limit $\beta = (\gamma - 1)/\gamma$ and small as $\beta \to 0$, then one may reasonably expect the error incurred in using the local similarity approximation to be quite small for all values of $\mathcal{H}$. Figs. 3b and 3c show the variation of the quantity $(\beta/Q_i)(dQ_i/d\beta)$ as a function of β, with $Q_i = f_w''$ and I_1, for several choices of the remaining similarity variables. It is apparent from these figures that the concept of local similarity should have a large range of application in treating viscous interaction problems.

In summary, it has been shown that the concept of local similarity has a firm analytic justification. By using the similar solution corresponding to the *local* value of β, the

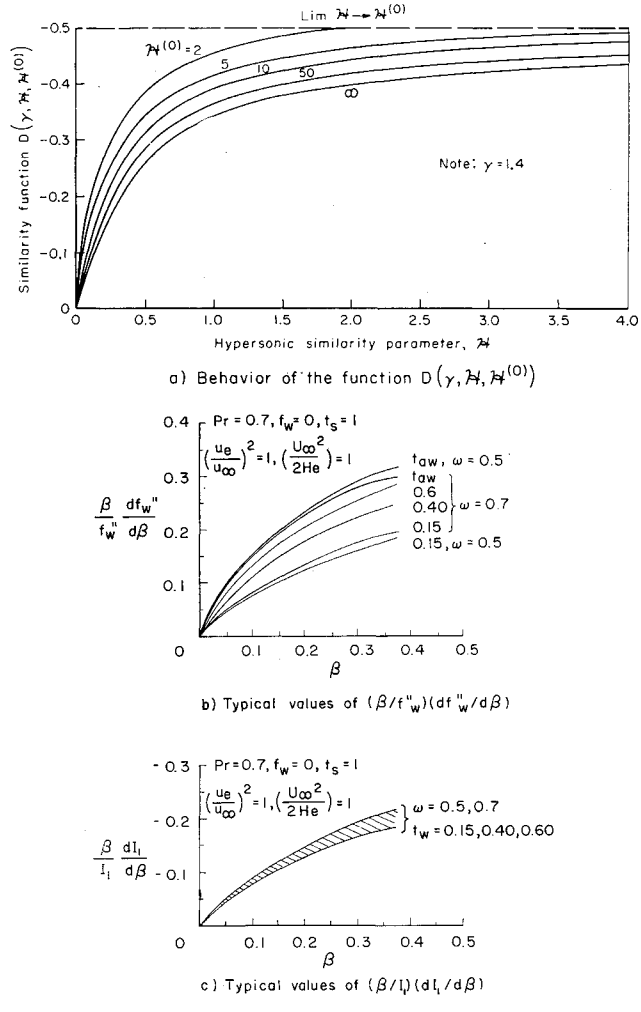

Fig. 3 Functions for use in evaluating the local similarity criteria

Table 2 Similar solutions for $Pr = 0.7$ and $f_w = 0$

β	ω	t_s	$(U_\infty^2/2H_e)(u_e/u_\infty)^2$		t_w	f_w''	θ_w'	g_w'	I_1	I_2	$I_1(1)$	$I_1(2)$	$I_1(3)$
0	1	all	1[a]	...	0.15	0.4696	0.3339	0.4696	0.6097	0.4696	1.686	1.686	1.267
					0.40	0.4696	0.3006	0.4696	0.9560	0.4696	1.686	1.686	1.217
					0.60	0.4696	0.2439	0.4696	1.233	0.4696	1.686	1.686	1.134
					0.8357	0.4696	0.0	0.4696	1.559	0.4696	1.686	1.686	0.7728
			0[a]	...	0.0[a]	0.4696	0.4139	0.4696	0.4696	0.4696	1.686	1.686	1.385
					1.0[b]	0.4696	0.4139	0.4696	1.686	0.4696	1.686	1.686	1.385
	0.7	all	1[a]	...	0.15	0.4450	0.3137	0.4450	0.5784	0.4449	1.586	1.586	1.186
					0.40	0.4834	0.3026	0.4834	0.9650	0.4833	1.681	1.681	1.193
					0.60	0.4956	0.2433	0.4956	1.262	0.4954	1.709	1.709	1.117
					0.8191	0.5033	0.0	0.5033	1.583	0.5031	1.726	1.726	0.7897
	0.5	all	1[a]	...	0.15	0.4325	0.3025	0.4325	0.5547	0.4309	1.524	1.524	1.141
					0.40	0.4979	0.3049	0.4979	0.9593	0.4940	1.676	1.676	1.195
					0.60	0.5198	0.2405	0.5198	1.262	0.5143	1.722	1.722	1.149
					0.8013	0.5341	0.0	0.5341	1.549	0.5245	1.743	1.743	0.9754
			0.5[a]	...	0.15	0.3734	0.2963	0.3734	0.4607	0.3734	1.452	1.452	1.166
					0.40	0.4394	0.3341	0.4394	0.8600	0.4394	1.610	1.610	1.250
					0.60	0.4642	0.3246	0.4642	1.167	0.4642	1.663	1.663	1.240
					0.9151	0.4876	0.0	0.4876	1.645	0.4876	1.710	1.710	0.7665
			0[a]	...	0.15	0.3490	0.3034	0.3490	0.4038	0.3490	1.411	1.411	1.185
					0.40	0.4143	0.3625	0.4143	0.7886	0.4143	1.571	1.571	1.303
					0.60	0.4399	0.3861	0.4399	1.089	0.4399	1.626	1.626	1.343
					1.0[b]	0.4696	0.4139	0.4139	1.686	0.4696	1.686	1.686	1.385
0.1	1	1	1	1	0.15	0.5085	0.3381	0.4781	0.5562	0.4529	1.660	1.610	1.240
					0.40	0.5331	0.3051	0.4824	0.8715	0.4460	1.647	1.576	1.174
					0.60	0.5525	0.2459	0.4857	1.121	0.4404	1.638	1.549	1.071
					0.8290	0.5744	0.0	0.4894	1.403	0.4341	1.627	1.520	0.6798
	0.7	1	1	1	0.15	0.4850	0.3206	0.4573	0.5307	0.4319	1.571	1.521	1.165
					0.40	0.5492	0.3097	0.5007	0.8833	0.4608	1.655	1.567	1.155
					0.60	0.5808	0.2466	0.5164	1.151	0.4655	1.674	1.575	1.059
					0.8123	0.6083	0.0	0.5274	1.430	0.4652	1.682	1.561	0.6985
		0.6250	1	1	0.15	0.5056	0.3237	0.4615	0.5274	0.4212	1.559	1.479	1.155
					0.8136	0.6652	0.0	0.5373	1.413	0.4391	1.656	1.466	0.6676
		0.3333	1	1	0.15	0.5523	0.3304	0.4188	0.5200	0.3963	1.531	1.387	1.133
					0.8161	0.7918	0.0	0.5580	1.378	0.3787	1.603	1.264	0.6103
	0.5	1	1	1	0.15	0.4731	0.3112	0.4473	0.5112	0.4202	1.515	1.466	1.123
					0.40	0.5650	0.3137	0.5186	0.8816	0.4730	1.658	1.578	1.160
					0.60	0.6059	0.2488	0.5441	1.158	0.4854	1.697	1.595	1.092
					0.7966	0.6372	0.0	0.5605	1.422	0.4895	1.715	1.593	0.8407
0.2	1	1	1	1	0.15	0.5242	0.3414	0.4851	0.5142	0.4395	1.639	1.550	1.219
					0.40	0.5883	0.3085	0.4926	0.8065	0.4270	1.618	1.491	1.141
					0.60	0.6241	0.2469	0.4983	1.036	0.4170	1.602	1.446	1.024
					0.8235	0.6633	0.0	0.5044	1.288	0.4057	1.586	1.397	0.6167
		0.6250	1	1	0.15	0.5840	0.3475	0.4935	0.5082	0.4214	1.615	1.475	1.199
					0.8257	0.7701	0.0	0.5215	1.260	0.3670	1.540	1.251	0.5735
		0.3333	1	1	0.15	0.6768	0.3604	0.5112	0.4959	0.3793	1.566	1.316	1.160
					0.8297	1.001	0.0	0.5550	1.207	0.2769	1.458	0.9577	0.4981
	0.7	1	1	1	0.15	0.5202	0.3265	0.4678	0.4929	0.4216	1.560	1.470	1.149
					0.40	0.6067	0.3154	0.5151	0.8198	0.4427	1.636	1.496	1.127
					0.60	0.6547	0.2488	0.5333	1.067	0.4413	1.651	1.473	1.015
					0.8066	0.6980	0.0	0.5464	1.316	0.4348	1.654	1.439	0.6360
		0.6250	1	1	0.15	0.5581	0.3319	0.4752	0.4878	0.4020	1.539	1.397	1.132
					0.8088	0.8005	0.0	0.5627	1.292	0.3874	1.612	1.281	0.5918
		0.3333	1	1	0.15	0.6428	0.3432	0.4908	0.4772	0.3566	1.495	1.239	1.098
					0.8125	1.024	0.0	0.5951	1.245	0.2777	1.535	0.9542	0.5150
	0.5	1	1	1	0.15	0.5089	0.3188	0.4601	0.4769	0.4118	1.509	1.420	1.109
					0.40	0.6239	0.3212	0.5363	0.8213	0.4560	1.646	1.502	1.134
					0.60	0.6814	0.2480	0.5646	1.077	0.4617	1.680	1.496	1.049
					0.7912	0.7268	0.0	0.5830	1.313	0.4595	1.694	1.475	0.7744
		0.6250	1	1	0.15	0.5440	0.3235	0.4666	0.4732	0.3919	1.491	1.350	1.094

momentum equation is satisfied identically to $0(\epsilon)$, provided that

$$\xi^{m+1}\frac{d^{m+1}\beta}{d\xi^{m+1}} \ll \xi^m \frac{d^m\beta}{d\xi^m} \qquad m = 1, 2, \ldots$$

The perturbation equation (67) may be solved numerically if an explicit value for the first-order correction is desired. Since $f_1 = f_1(\beta; \eta)$, the solutions will be universal functions and, like the zero-order similar solutions, may be computed once and for all for any combination of similarity parameters.

VI Comparison With Experiment

In the previous section, a procedure for calculating the local surface pressure, heat transfer, and skin friction for all values of the interaction parameter χ_∞ was described. The method requires that the quantities I_1, f_w'', g_w', and θ_w' be known as a function of the similarity parameters t_w, t_s, $U_\infty^2/2H_e$, u_e/u_∞, β, f_w, and the viscosity-temperature relation and Pr. To express the viscosity-temperature relation in parametric form, one may either follow the approach of Crocco[29] in using Sutherland's law or assume that $\mu \sim T^\omega$, where

Table 2 (*Continued*)

β	ω	t_s	$(U_\infty^2/2H_e)$	$(u_e/u_\infty)^2$	t_w	f_w''	θ_w'	g_w'	I_1	I_2	$I_1(1)$	$I_1(2)$	$I_1(3)$
					0.7936	0.8245	0.0	0.5979	1.296	0.4092	1.659	1.316	0.7203
		0.3333	1	1	0.15	0.6230	0.3337	0.4807	0.4642	0.3450	1.453	1.196	1.062
					0.7972	1.040	0.0	0.6287	1.256	0.2919	1.590	0.9806	0.6430
0.2857	0.7	1	1	1	0.15	0.5475	0.3310	0.4758	0.4660	0.4143	1.553	1.433	1.138
					0.40	0.6512	0.3195	0.5259	0.7751	0.4297	1.625	1.439	1.107
					0.60	0.7119	0.2501	0.5458	1.008	0.4239	1.635	1.402	0.9849
					0.8025	0.7665	0.0	0.5603	1.238	0.4130	1.635	1.355	0.5953
		0.6250	1	1	0.15	0.5984	0.3379	0.4853	0.4601	0.3882	1.526	1.339	1.117
					0.8051	0.9029	0.0	0.5806	1.211	0.3498	1.585	1.155	0.5448
		0.3333	1	1	0.15	0.7115	0.3521	0.5050	0.4480	0.3276	1.473	1.139	1.075
					0.8095	1.198	0.0	0.6200	1.160	0.2040	1.496	0.7499	0.4597
	0.5	1	1	1	0.15	0.5370	0.3246	0.4700	0.4522	0.4059	1.506	1.387	1.100
					0.40	0.6697	0.3269	0.5497	0.7788	0.4438	1.639	1.448	1.115
					0.60	0.7398	0.2502	0.5800	1.020	0.4445	1.670	1.428	1.019
					0.7872	0.7955	0.0	0.5999	1.237	0.4378	1.680	1.394	0.7 49
		0.6250	1	1	0.15	0.5843	0.3307	0.4784	0.4478	0.3791	1.483	1.296	1.080
					0.7901	0.9259	0.0	0.6185	1.219	0.3704	1.639	1.191	0.6689
		0.3333	1	1	0.15	0.6899	0.3436	0.4963	0.4374	0.3161	1.436	1.098	1.042
					0.7945	1.211	0.0	0.6562	1.176	0.2129	1.558	0.7672	0.5 82
0.4	1	1	1	1	0.15	0.5998	0.3465	0.4959	0.4515	0.4192	1.608	1.460	1.187
					0.40	0.6824	0.3134	0.5082	0.7109	0.3980	1.575	1.366	1.092
					0.60	0.7461	0.2474	0.5173	0.9129	0.3809	1.552	1.295	0.9563
					0.8147	0.8125	0.0	0.5264	1.125	0.3624	1.529	1.224	0.5334
				0.5[d]	0.15	0.5948	0.3901	0.4942	0.4156	0.4286	1.614	1.487	1.261
					0.9074	0.8337	0.0	0.5282	1.173	0.3645	1.525	1.221	0.5248
				0[d]	0.15	0.5901	0.4327	0.4926	0.3806	0.4379	1.619	1.514	1.333
					1.0[c]	0.8544	0.0	0.5300	1.219	0.3667	1.521	1.219	1.257
		0.6250	1	1	0.15	0.6727	0.3563	0.5094	0.4438	0.3887	1.571	1.342	1.158
					0.8179	0.9951	0.0	0.5520	1.091	0.2967	1.467	1.006	0.4799
		0.3333	1	1	0.15	0.8319	0.3759	0.5366	1.4288	0.3173	1.500	1.098	1.103
					0.8231	1.383	0.0	0.5993	1.033	0.1439	1.363	0.5815	0.3953
	0.7	1	1	1	0.15	0.5807	0.3363	0.4853	0.4361	0.4062	1.546	1.393	1.126
					0.40	0.7054	0.3244	0.5385	0.7256	0.4151	1.613	1.377	1.085
					0.60	0.7813	0.2515	0.5604	0.9432	0.4041	1.620	1.324	0.9519
					0.7977	0.8491	0.0	0.5762	1.153	0.3882	1.618	1.264	0.5493
				0.5[d]	0.15	0.5281	0.3422	0.4344	0.3749	0.3781	1.475	1.366	1.166
					0.9058	0.8470	0.0	0.5430	1.186	0.3729	1.551	1.235	0.5241
				0[d]	0.15	0.5027	0.3597	0.4129	0.3347	0.3688	1.443	1.358	1.204
					1.0[c]	0.8544	0.0	0.5300	1.219	0.3667	1.521	1.219	1.257
		0.6250	1	1	0.15	0.6473	0.3449	0.4971	0.4295	0.3725	1.513	1.275	1.100
					0.8231	1.025	0.0	0.6007	1.123	0.3070	1.559	1.020	0.4972
				0.5	0.15	0.6049	0.3457	0.4564	0.3834	0.3595	1.456	1.272	1.126
					0.8763	1.032	0.0	0.5743	1.136	0.3045	1.502	1.013	0.4875
				0	0.15	0.5807	0.3550	0.4369	0.3527	0.3550	1.429	1.274	1.152
					0.9414	1.040	0.0	0.5619	1.152	0.3028	1.475	1.008	0.5242
		0.3333	1	1	0.15	0.7938	0.3622	0.5212	0.4163	0.2943	1.450	1.029	1.051
					0.8057	1.404	0.0	0.6472	1.071	0.1195	1.459	0.5313	0.4073
				0.5	0.15	0.7613	0.3602	0.4911	0.3840	0.3004	1.406	1.055	1.065
					0.8545	1.418	0.0	0.6275	1.070	0.1347	1.414	0.5586	0.4055
				0	0.15	0.7382	0.3634	0.4742	0.3620	0.3038	1.385	1.071	1.081
					0.8964	1.428	0.0	0.6161	1.072	0.1049	1.390	0.5695	0.4242
	0.5	1	1	1	0.15	0.5712	0.3317	0.4821	0.4245	0.3933	1.503	1.350	1.089
					0.40	0.7258	0.3336	0.5659	0.7308	0.4298	1.632	1.388	1.096
					0.60	0.8111	0.2526	0.5986	0.9568	0.4249	1.660	1.352	0.9868
					0.7829	0.8787	0.0	0.6195	1.157	0.4132	1.669	1.305	0.6800
				0.5[d]	0.15	0.4887	0.3141	0.3992	0.3511	0.3483	1.394	1.296	1.111
					0.9048	0.8563	0.0	0.5533	1.194	0.3786	1.570	1.244	0.5234
				0[d]	0.15	0.4540	0.3192	0.3686	0.3094	0.3303	1.347	1.273	1.133
					1.0[c]	0.8544	0.0	0.5300	1.219	0.3667	1.521	1.219	1.257
		0.6250	1	1	0.15	0.6332	0.3393	0.4926	0.4197	0.3645	1.477	1.236	1.066
					0.7859	1.048	0.0	0.6234	1.134	0.3259	1.620	1.054	0.6163
				0.5	0.15	0.5674	0.3221	0.4255	0.3616	0.3359	1.383	1.213	1.077
					0.8738	1.044	0.0	0.5893	1.149	0.3086	1.530	1.019	0.4873
				0	0.15	0.5342	0.3219	0.3972	0.3279	0.3244	1.342	1.204	1.092
					0.9407	1.044	0.0	0.5669	1.156	0.3040	1.484	1.009	0.5240
		0.3333	1	1	0.15	0.7705	0.3550	0.5144	0.4079	0.2829	1.420	0.9910	1.022
					0.7909	1.414	0.0	0.6869	1.090	0.1222	1.529	0.5369	0.5194
				0.5	0.15	0.7224	0.3403	0.4643	0.3656	0.2836	1.346	1.012	1.022
					0.8498	1.431	0.0	0.6476	1.087	0.1264	1.452	0.5408	0.4056
				0	0.15	0.6910	0.3363	0.4393	0.3396	0.2835	1.311	1.024	1.030
					0.8938	1.434	0.0	0.6268	1.081	0.1360	1.410	0.5589	0.4240

[a] Applies to all cases where the product $\sigma_1 = (U_\infty^2/2H_e)[(u_e/u_\infty)^2 \cos^2\Lambda + \sin^2\Lambda]$ has the same value.
[b] All quantities linear in t_w.
[c] These values correct for all ω.
[d] Applies to all cases where the product $\sigma_2 = (U_\infty^2/2H_e)(u_e/u_\infty)^2$ has the same value.

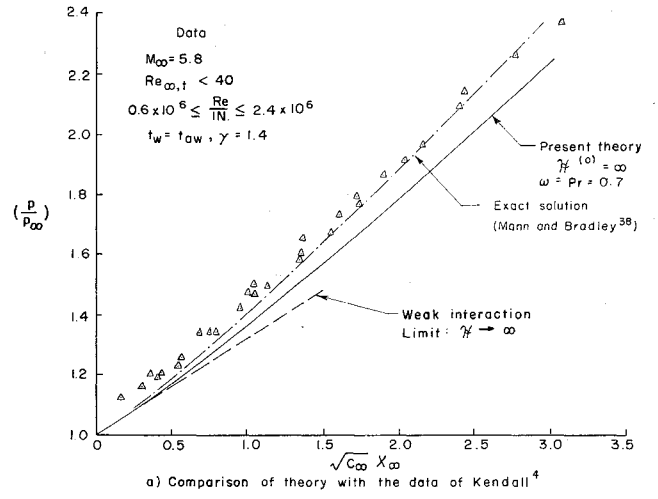

a) Comparison of theory with the data of Kendall[4]

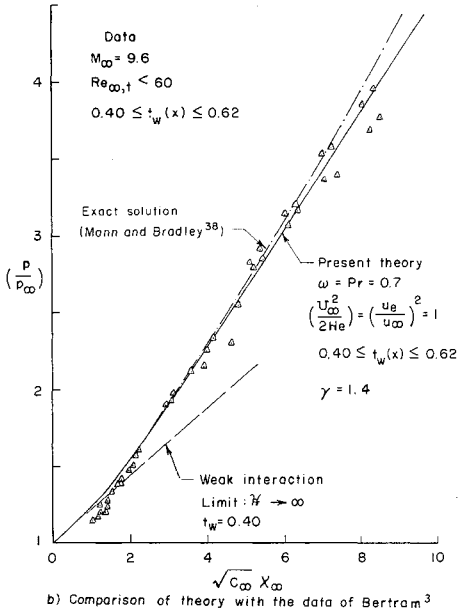

b) Comparison of theory with the data of Bertram[3]

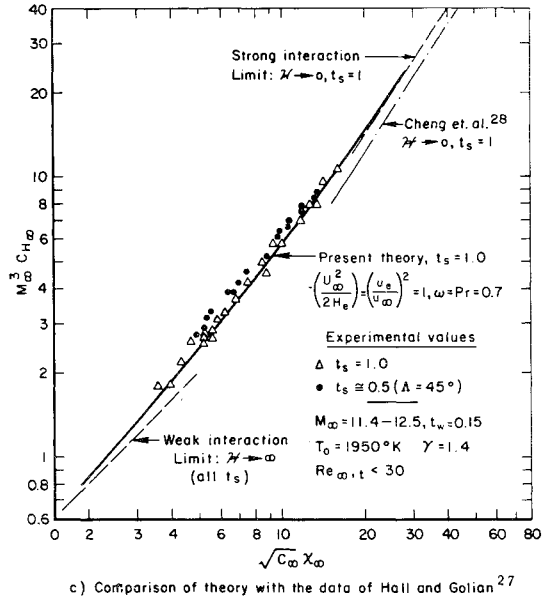

c) Comparison of theory with the data of Hall and Golian[27]

Fig. 4 Comparison of the local similarity solution with experimental data

ω is a constant. In view of the fact that Sutherland's law itself represents an approximation to the intermolecular potential, the power law variation of viscosity appears to be equally suitable to the parameterization requirements and offers certain conceptual advantages when dealing with air and other gases at high temperature.[||] The Prandtl number was taken to be a constant; this approximation is quite justified over the complete range of temperature and pressure for which the gas remains undissociated.[33]

The numerical results tabulated in the Appendix represent a small portion of the similarity solutions that will be available shortly.[32] The selected values given here should be sufficient to cover the majority of cases where viscous interaction occurs with a perfect gas. In the literature, a certain amount of numerical confusion has resulted from the fact that the limiting theories for strong and weak interaction have been compared with experimental data using inappropriate solutions to the similarity equations. The reasons for this are partly historical (only recently has the number of these solutions increased significantly [6,13–15,29,31,33–35]) and partly heuristic; in most cases, the agreement between theory and experiment is considerably better if the correct similarity solutions are used in interpreting the theory.

A comparison of the present theory with heat transfer and surface pressure data is given in Fig. 4. Of the several available sets of measurements, those of Hall and Golian,[27] Kendall,[4] and Bertram[3] were judged to be the most accurate while at the same time exhibiting the basic features of the region between the strong and weak interaction limits.

In Fig. 4a, the data of Kendall are compared with the present theory using $\mathcal{H}^{(0)} = \infty (\alpha = 0)$. The theory lies about 8% below the experimental values but agrees qualitatively over the whole range of χ_∞ investigated. Also included in figure are the recent calculations of Mann and Bradley.[44] Their numerical solution is accomplished using the exact (nonsimilar) boundary layer equations and the method of characteristics for the inviscid flow. Their method requires an iteration between the characteristics and boundary layer computations until a self-consistent viscous-inviscid flow field is obtained.

The data of Bertram[3] were obtained with a flat plate whose temperature was less than the insulated value t_{aw} and varied in the streamwise direction as shown in Fig. 8 of Ref. 3. As described earlier, the extension of local similarity to situations where the surface temperature varies means that $I_1 = I_1(\chi_\infty, \mathcal{H})$ and Eqs. (55) and (56) must be solved simultaneously by iteration. That this iteration process is strongly convergent and easily applied is attested to by the fact that the curve of Fig. 4b required only two iterations (and 1 hr of hand computation) to converge to three-figure accuracy. The present theory is in substantial agreement with Bertram's data for $C_\infty^{1/2}\chi_\infty > 2$. Below this value, the experiments may be subject to some uncertainty (see Ref. 3, p. 13). The exact solution of Mann and Bradley[44] and the present theory are in excellent agreement for this experiment.

Fig. 4c compares the results of the present theory with the heat transfer data of Hall and Golian.[27] The range of $C_\infty^{1/2}\chi_\infty$, from 4 to 20, lies between the strong and weak interaction limits. For the unyawed plate, the present theory shows excellent agreement with experiment. In the limit of $\mathcal{H} \to \infty$, both the yawed and unyawed cases should give identical results; in the limit of $\mathcal{H} \to 0$, the present theory predicts a value $M_\infty^3\, C_{H_\infty}$ for $t_s = 0.5$ about 1.86% higher than the corresponding case with $t_s = 1$. In contrast, the data for $t_s = 0.5$ are about 6% higher than the unyawed values at $C_\infty^{1/2}\chi_\infty = 13.5$, and the differences increase with decreasing $C_\infty^{1/2}\chi_\infty$. Flügge-Lotz and Blottner[45] have carried out exact

[||] Van Driest (see Ref. 29) shows considerable differences between the solutions obtained using the Sutherland and power-law relations for viscosity. However, if a realistic choice is made for ω, the differences are negligible.

Table 3 Similar solutions with surface mass transfer, $Pr = 0.7$ and $t_s = 1$

β	ω	f_w	σ_2[a]	t_w	f_w''	θ_w'	g_w'	I_1	I_2	$I_1(1)$	$I_1(2)$	$I_1(3)$
0	0.7	−0.2	1	0.15	0.3050	0.2205	0.3050	0.6634	0.5049	1.902	1.902	1.457
				0.7930	0.3611	0.0	0.3611	1.761	0.5608	2.012	2.013	1.212
		−0.4	1	0.15	0.1795	0.1369	0.1795	0.7838	0.5794	2.374	2.374	1.871
				0.7625	0.2310	0.0	0.2310	2.004	0.6306	2.416	2.416	1.734
		−0.6	1	0.15	0.0745	0.0651	0.0745	0.9822	0.6741	3.216	3.216	2.628
				0.7262	0.1175	0.0	0.1175	2.377	0.7168	3.506	3.506	2.478
	0.5	−0.2	1	0.15	0.2916	0.2092	0.2916	0.6378	0.4899	1.839	1.839	1.413
				0.7777	0.3886	0.0	0.3886	1.717	0.5806	2.012	2.012	1.327
		−0.4	1	0.15	0.1660	0.1261	0.1660	0.7559	0.5632	2.322	2.322	1.842
				0.7474	0.2550	0.0	0.2550	1.923	0.6455	2.379	2.379	1.804
		−0.6	1	0.15	0.0624	0.0553	0.0624	0.9630	0.6578	3.239	3.239	2.677
				0.7125	0.1370	0.0	0.1370	2.230	0.7236	2.940	2.940	2.470
0.2	0.7	−0.2	1	0.15	0.3846	0.2361	0.3329	0.5484	0.4749	1.837	1.724	1.383
				0.7768	0.5615	0.0	0.4121	1.410	0.4795	1.880	1.627	0.9754
		−0.4	1	0.15	0.2633	0.1562	0.2135	0.6187	0.5395	2.213	2.070	1.707
				0.7404	0.4353	0.0	0.2910	1.513	0.5326	2.165	1.866	1.357
		−0.6	1	0.15	0.1610	0.0896	0.1149	0.7117	0.6185	2.753	2.569	2.185
				0.6954	0.3220	0.0	0.1865	1.629	0.5961	2.530	2.176	1.797
	0.5	−0.2	1	0.15	0.3731	0.2286	0.3247	0.5311	0.4645	1.782	1.672	1.342
				0.7640	0.5874	0.0	0.4456	1.402	0.5028	1.910	1.655	1.071
		−0.4	1	0.15	0.2523	0.1493	0.2053	0.6011	0.5288	2.159	2.020	1.670
				0.7298	0.4579	0.0	0.3209	1.490	0.5530	2.171	1.878	1.438
		−0.6	1	0.15	0.1515	0.0838	0.1078	0.6955	0.6080	2.710	2.531	2.160
				0.6897	0.3406	0.0	0.2108	1.601	0.6135	2.514	2.169	1.831

[a] $\sigma_2 = (U_\infty^2/2He)(ue/u_\infty)^2$.

numerical solutions for this problem in a manner similar to that of Mann and Bradley. Their results lie 10 to 20% below both the experimental values and the present theory.

In Fig. 4c, the theory of Cheng et al.[28] for the strong interaction region also is shown. This theory predicts a value $M_\infty^3 C_{H\infty}$ about 14% too low ($\gamma = 1.4$); considering the fact that bluntness also may be taken into account using Cheng's result, this discrepancy does not appear to be too serious.

It should be emphasized that, in the present approach, there is no necessity to distinguish between strong and weak interaction, with one formulation being used for all values of the interaction parameter χ_∞; furthermore, there are no approximations required beyond those leading to Eqs. (54) and (56), and the use of adjustable constants is eliminated by taking the exact values of I_1, θ_w', and f_w'' directly from the appropriate solutions to the similarity equations. The *local* similarity solution is shown to satisfy the exact momentum equation to $0(\epsilon)$, and the error incurred may be estimated as $0(\Psi)$ [see Eq. (51)]. It is in the foregoing respects that the present theory differs most significantly from other recent applications of local similarity concepts to viscous interaction problems.[6,37]

Appendix: Similar Solutions of the Laminar Boundary Layer Equations

Proper interpretation of any theory involving the laminar boundary layer ultimately requires a numerical solution of the governing equations. The Howarth-Dorodnitsyn transformation may be applied in certain restricted circumstances; this results in a series of coupled nonlinear ordinary differential equations that may be normalized and solved once and for all for any given combination of boundary conditions and governing parameters. Further simplifications, such as taking the $\rho\mu$ product to be constant and the Prandtl number to be unity, may reduce the mathematical difficulties but are not essential.

The present solutions[32] to Eqs. (16, 17, and 29) were obtained using an IBM 7090 high speed computing machine and are given in Tables 1–3. This type of two-point boundary value problem is most easily solved by assuming values for the derivatives f_w'', θ_w', and g_w' and numerically integrating the equations across the boundary layer. If the boundary conditions on f', θ, and g for $\eta \to \infty$ are not satisfied to sufficient accuracy, new estimates for f_w'', θ_w', and g_w' are made and the calculation repeated until proper convergence is obtained. A Runge-Kutta scheme was used to integrate the differential equations from $\eta = 0$ to $\eta = 10.0$, using an interval of 0.1 in η. Several available numerical solutions[10,15] were compared to the present calculations, and in all cases agreement was obtained to four significant figures.

Of particular interest is the method of improving successive guesses on f_w'', θ_w', and g_w' such that the solution converges to the specified boundary conditions at the outer edge of the boundary layer. To this end, special techniques were developed by Katherine Purdom# of the Rand Corporation. Beginning with a set of initial values for f_w'', θ_w', and g_w', the integration is repeated four times: first using the initial values as given, and subsequently with one of the three derivatives changed by a small amount. The results of these four computations represent a set of equations that are solved using the Newton-Rhapson method for the roots yielding the correct boundary conditions. The roots obtained are used as new guesses for f_w'', θ_w', and g_w', and the process is repeated until successive values of the three derivatives differ by less than 0.00001. The success of this method is attested to by the fact that f_w'', θ_w', and g_w' converged to within 0.00001 in about four iterations, even though the initial guesses differed by 20% from the final answers. For the insulated wall ($\theta_w' = 0$), a double iteration procedure was used to determine the value of t_{aw}. The value of t_{aw} is believed to be accurate to 0.00001. Although the Blasius values of $\theta_w' = f_w'' = 0.4696$ and $t_{aw} = 1$ are in general agreement with the present results, differences of 20 to 50% are not uncommon. From the numerical results, it readily may be seen that the sweep parameter t_s has a negligible influence on the wall derivatives, a result that also was obtained by Whelan[33] for $\omega = 1$ and $Pr = 1$.

In addition to the derivatives f_w'', θ_w', and g_w' appearing in the skin friction and heat transfer relations, certain integrals also are useful in determining the boundary layer profile parameters. Two of these, I_1 and I_2, are defined by Eqs.

Now with Lockheed Missiles and Space Division, Palo Alto, Calif.

(48) and (49). They may be written

$$I_1 = (1 - t_s)[I_1(1) - I_1(2)] - (1 - t_w)I_1(3) + I_1(2) \quad \text{(A1)}$$

$$I_2 = \int_0^\infty f'(1 - f')d\eta$$

where

$$I_1(1) = \int_0^\infty (1 - g^2)\, d\eta$$

$$I_1(2) = \int_0^\infty (1 - f'^2)\, d\eta \quad \text{(A2)}$$

$$I_1(3) = \int_0^\infty (1 - \theta)\, d\eta$$

Since the last three integrals are often useful in themselves (cf., Ref. 15), they have been included in the tabulation.

Acknowledgments

It is a pleasure to acknowledge the assistance and encouragement of Joseph F. Gross, Carl Gazley Jr., and E. P. Williams of the Rand Corporation. The author wishes to thank Toshi Kubota of the California Institute of Technology for many valuable discussions of this problem. Special credit is due Katherine Purdom for developing the numerical techniques used to solve the boundary layer similarity equations.

References

[1] Lees, L. and Probstein, R. F., "Hypersonic flows of a viscous fluid," Princeton Monograph (1953).

[2] Li, T. Y. and Nagamatsu, H. T., "Shock-wave effects on the laminar skin friction of an insulated flat plate at hypersonic speeds," J. Aeronaut. Sci. **20**, 345–355 (1953).

[3] Bertram, M. H., "Boundary-layer displacement effects in air at Mach numbers of 6.8 and 9.6," NASA TR R-22 (1959).

[4] Kendall, J. M., Jr., "An experimental investigation of leading edge shock wave—boundary layer interaction at Mach 5.8," J. Aeronaut. Sci. **24**, 47–56 (1957).

[5] Lees, L., "Laminar heat transfer over blunt-nosed bodies at hypersonic flight speeds," Jet Propulsion **26**, 259–269 (1956).

[6] Kemp, N. H., Rose, P. H., and Detra, R. W., "Laminar heat transfer around blunt bodies in dissociated air," J. Aero/Space Sci. **26**, 421–430 (1959).

[7] Low, G. M., "The compressible laminar boundary layer with fluid injection," NACA TN 3404 (1955).

[8] Brown, W. B. and Donoughe, P. L., "Tables of exact laminar boundary-layer solutions when the wall is porous and fluid properties are variable," NACA TN 2479 (1951).

[9] Mickley, H. S., Ross, R. C., Squyers, A. L., and Stewart, W. E., "Heat, mass, and momentum transfer for flow over a flat plate with flowing or suction," NACA TN 3208 (1954).

[10] Emmonds, H. W. and Leigh, D., "Tabulation of the Blasius function with blowing and suction," Harvard Univ. Combustion Aeronaut. Lab. Interim TR 9 (1953).

[11] Gross, J. F., Hartnett, J. P., Masson, D. J., and Gazley, C., Jr., "A review of binary laminar layer boundary layer characteristics," Internatl. J. Heat Mass Transfer **3**, 198–222 (1961).

[12] Lees, L., "Convective heat transfer with mass addition and chemical reactions," *Combustion and Propulsion, Third AGARD Colloquium* (Pergamon Press, New York, 1958), pp. 451–498.

[13] Li, T. Y. and Gross, J. F., "Hypersonic strong viscous interaction on a flat plate with surface mass transfer," *Proceedings of the 1961 Heat Transfer and Fluid Mechanics Institute* (Stanford University Press, Stanford, Calif., 1961), pp. 146–160.

[14] Reshotko, E. and Beckwith, I. E., "Compressible laminar boundary layer over a yawed infinite cylinder with heat transfer and arbitrary Prandtl number," NACA Rept. 1379 (1958); supercedes NACA TN 3986 (1957).

[15] Beckwith, I. E., "Similar solutions for the compressible boundary layer on a yawed cylinder with transpiration cooling," NASA TR R-42 (1959); supercedes NACA TN 4345 (1958).

[16] Charwat, A. F., "Tentative generalization of leading-edge viscous interaction phenomena," Rand Publ. P-1994 (1960).

[17] Cole, J. D., "Sweepback theory for shock waves at hypersonic speeds," Rand Publ. P-1337 (1958).

[18] Oguchi, H., "First-order approach to a strong interaction problem in hypersonic flow over an insulated flat plate," Univ. Tokyo, Aeronaut. Research. Inst. Rept. 330 (1958).

[19] Feldman, S., "Hypersonic gas dynamic charts for equilibrium air," Avco Research Lab. (1957).

[20] Nagamatsu, H. T. and Sheer, R. E., Jr., "Hypersonic shock wave-boundary layer interaction and leading edge slip," ARS J. **31**, 902–910 (1961).

[21] Van Dyke, M., "Reviews," J. Fluid Mech. **8**, 320 (1960).

[22] Hayes, W. D. and Probstein, R. F., *Hypersonic Flow Theory* (Academic Press, New York, 1959), pp. 333–367.

[23] Lees, L., "On the boundary-layer equations in hypersonic flow and their approximate solutions," J. Aeronaut. Sci. **20**, 143–145 (1953).

[24] Nagamatsu, H. T., Weil, H. A., and Sheer, R. E., Jr., "Heat transfer to flat plate in high temperature rarefied ultra-high Mach number flow," ARS J. **32**, 533–541 (1962).

[25] Aeroesty, J., "Pressure distributions on flat plates at Mach 4 and low density flow," Univ. Calif., Inst. Eng. Research Rept. HE-150-157 (1958).

[26] Oguchi, H., "The sharp leading edge problem in hypersonic flow," Brown Univ., Div. of Eng. Rept. ARL TN 60-133 (1960).

[27] Hall, J. G. and Golian, T. C., "Heat transfer to sharp and blunt yawed plates in hypersonic airflow," Cornell Aeronaut. Lab. Rept. AD-1052-A-11 (1960).

[28] Cheng, H. K., Hall, J. G., Golian, T. C., and Hertzberg, A., "Boundary-layer displacement and leading-edge bluntness effects in high-temperature hypersonic flow," J. Aeronaut. Sci. **28**, 353–381, 410 (1961).

[29] Crocco, L., "Lo strato limite laminare nei gas," Monograf. Sci. Aeronaut. 3, Ministero della Difesa-Aeronaut., Rome (1946); also Van Driest, E. R., "Investigation of laminar boundary layer in compressible fluids using the Crocco method," NACA TN 2597 (1952).

[30] Cohen, N. B., "Correlation formulas and tables of density and some transport properties of equilibrium dissociating air for use in solutions of the boundary-layer equations," NASA TN D-194 (1960).

[31] Beckwith, I. E. and Cohen, N. B., "Application of similar solutions to calculation of laminar heat transfer on bodies with yaw and large pressure gradient in high-speed flow," NASA TN D-625 (1961).

[32] Gross, J. F. and Dewey, C. F., Jr., "A tabulation of exact solutions to the laminar boundary layer equations," Rand Corp. (to be published).

[33] Whelan, R. J., "Boundary-layer interaction on a yawed infinite wing in hypersonic flow," J. Aeronaut. Sci. **26**, 839–851 (1959).

[34] Fay, J. A. and Riddell, F. R., "Theory of stagnation point heat transfer in dissociated air," J. Aeronaut. Sci. **25**, 73–85, 121 (1958).

[35] Romig, M. F. and Dore, F. J., "Solutions of the compressible laminar boundary layer including the case of a dissociated free stream," Convair Rept. ZA-7-012 (1954).

[36] Moore, F. K., "On local flat-plate similarity in the hypersonic boundary layer," Cornell Aeronaut. Lab. Rept. AF-1285-A-2 (1961).

[37] Bertram, M. H. and Henderson, A., Jr., "Effects of boundary layer displacement and leading-edge bluntness on pressure distribution, skin friction, and heat transfer of bodies at hypersonic speeds," NACA TN 4301 (1958); also Bertram, M. H. and Feller, W. V., "A simple method for determining heat transfer, skin friction, and boundary-layer thickness for hypersonic laminar boundary-layer flows in a pressure gradient," NASA Memo. 5-24-59L (1959); also Bertram, M. H. and Blackstock, T. A., "Some simple solutions to the problem of predicting boundary-layer self-induced pressures," NASA TN D-798 (1961).

[38] Liu, J. T. C., "On the role of high-temperature effects on heat transfer in hypersonic viscous interaction," *Developments in Mechanics* (Plenum Press, New York, 1961), Vol. 1.

[39] Mirels, H., "Approximate analytical solutions for hypersonic flow over slender power law bodies," NASA TR R-15 (1959).

[40] Mirels, H. and Thornton, P. R., "Effect of body perturbations on hypersonic flow over slender power law bodies," NASA TR R-45 (1959).

[41] Aroesty, J., "Strong interaction with slip boundary conditions," Aeronaut. Research Labs. Rept. 64 (1961).

[42] Görtler, H., "A new series for calculation of steady laminar boundary layer flows," J. Math. Mech. 6, 1–66 (1957).

[43] Merk, H. J., "Rapid calculations for boundary-layer transfer using wedge solutions and asymptotic expansions," J. Fluid Mech. 5, 460–480 (1959).

[44] Mann, W. M. and Bradley, R. G., Jr., "Hypersonic viscid-inviscid interaction solutions for perfect gas and equilibrium real air boundary layer flow," Am. Astronaut. Soc. Preprint 61-19 (January 1961).

[45] Flügge-Lotz, I. and Blottner, F. C., "Computation of the compressible laminar boundary-layer flow including displacement-thickness interaction using finite-difference methods," Stanford Univ. TR 131 (1962).

[46] Low, G. M., "The compressible laminar boundary layer with heat transfer and small pressure gradient," NACA TN 3028 (1953).

JANUARY 1963 AIAA JOURNAL VOL. 1, NO. 1

Second-Order Effects in Laminar Boundary Layers

STEPHEN H. MASLEN*

Martin Company, Baltimore, Md.

Second-order boundary layer disturbances are due to the displacement of the main flow by the boundary layer, surface curvature, freestream vorticity, and slip. A procedure for finding these is given for compressible flow of a perfect gas having a classically similar boundary layer. Solutions are given for the flat plate and circular cylinder and for the hypersonic axisymmetric stagnation point. For the latter flow, the dominant effect is that of vorticity, which increases both shear and heat flux. For the plate or cylinder, the same conclusion tends to hold for high speed flow. The vorticity effect is governed by the entire outer flow—not just the wall vorticity.

Nomenclature

a_1, c_1 = slip parameters, Eq. (17)
C_f = skin friction coefficient, Eq. (18a)
f, F, g, G = similarity functions, Eq. (9)
H = local stagnation enthalpy
K = constant, Eq. (9)
M = Mach number
Nu = Nusselt number, Eq. (18b)
P = pressure
Pr = Prandtl number
r = radial coordinate
R, R_0 = longitudinal radius of curvature; local and stagnation point, respectively
Re = Reynolds number, $\bar{\rho}\bar{u}\xi/\bar{\mu}$
T = temperature
u, v = velocity components along and normal to surface
x, z = distorted coordinates, Eq. (8)
γ = ratio of specific heats
Γ = profile function, Eq. (22a)
ϵ = small quantities depending on x, Eq. (9)
η = similarity variable, Eq. (8)
ζ, ξ = coordinates normal and tangent to surface
θ = $\cos^{-1}(dr_w/d\xi)$
λ_1 = function defined in Eq. (25a)
μ = viscosity
ρ = density
σ = 0 or 1 for plane or axisymmetric flow

Barred quantities are evaluated at the wall in the absence of viscosity.

Subscripts

e = conditions outside the boundary layer in its presence
w = wall
0 = first approximation

Use of a coordinate as a subscript indicates differentiation.

Presented at the ARS Space Flight Report to the Nation, New York, October 9–15, 1961; revision received November 14, 1962.

* Chief, Aerophysics Research, Research and Development Department. Member ARS.

Introduction

UNDER extreme conditions of fluid motion, particularly in very high speed flight at high altitude, the boundary layer near a surface can become sufficiently thick to affect materially the external flow. In turn, this influences the forces and heat transfer at the wall. At the same time and to the same order, roughly speaking, other assumptions of the classical boundary layer theory begin to break down.

The upshot is that four effects appear, all of order $Re^{-1/2}$, with respect to the classical results. These are due to the following: the boundary layer itself, nonuniformities in the external stream, curvature of the surface, and slip (in velocity and temperature) at the surface.

Two points of view can be taken. One is to consider a sharp leading edge and examine the flow "near" the edge, where the boundary layer exerts a considerable effect on the outer flow. This is the so-called "strong interaction" problem and it is not considered here. The other viewpoint, the subject of this discussion, involves weak interactions. One assumes that the boundary layer causes only small changes in the external flow. This is of interest near a blunt stagnation point and far back on a sharp-edged body.

Various aspects have been discussed by a number of authors. The self-induced effect of the boundary layer on a flat plate at high speed is described in Refs. 1–3, and at low speed in Refs. 1 and 4. The effect of freestream nonuniformities has been debated at length for the incompressible flat plate, for example, Refs. 5–10. The stream vorticity effect at a stagnation point is analyzed in Refs. 11–13. The effect of lateral curvature has been discussed by Probstein and Elliott,[14] whereas slip at the wall has been examined in Refs. 1, 15, and 16, among others.

A more complete general discussion of the stagnation point has been given by Lenard.[17] Finally, a general discussion of higher approximations has been given by Van Dyke[18,19] with particular reference to the flow near a stagnation point.

To the order currently of interest, questions of the form of the expansion (see, e.g., Goldstein[20]) or of optimal coordinates (Kaplun[21]) are not of concern. To second order (the first